Published in : International Journal of Pharmaceutics (2023), vol. 641, pp. 123088
DOI: 10.1016/j.ijpharm.2023.123088
Status : Postprint (Author's version)

PREFORMULATION STUDY FOR THE SELECTION OF A SUITABLE POLYMER FOR THE DEVELOPMENT OF ELLAGIC ACID-BASED SOLID DISPERSION USING HOT-MELT EXTRUSION

Isaïe Nyamba[a,b], Olivier Jennotte[a], Charles B. Sombié[b], Anna Lechanteur[a], Pierre-Yves Sacre[c], Abdoulaye Djandé[d], Rasmané Semdé[b], Brigitte Evrard[a]

[a]*Laboratory of Pharmaceutical Technology and Biopharmacy, Center for Interdisciplinary Research on Medicines (CIRM), Université de Liège, 4000 Liège, Belgium*
[b]*Laboratory of Drug Development, Center of Training, Research and Expertise in Pharmaceutical Sciences (CFOREM), Doctoral School of Sciences and Health, Université Joseph KI-ZERBO, 03 BP 7021 Ouagadougou 03, Burkina Faso*
[c]*Laboratory of Pharmaceutical Analytical Chemistry, Department of Pharmacy, Center for Interdisciplinary Research on Medicines (CIRM), University of Liege, 4000 Liege, Belgium*
[d]*Department of Chemistry, Laboratory of Molecular Chemistry and Materials, Research Team: Organic Chemistry and Phytochemistry, Université Joseph KI-ZERBO, 03 BP 7021 Ouagadougou 03, Burkina Faso*

Abstract

Ellagic acid is one of the most studied polyphenolic compounds due to its numerous promising therapeutic properties. However, this therapeutic potential remains difficult to exploit owing to its low solubility and low permeability, resulting in low oral bioavailability. In order to allow an effective therapeutic application of EA, it is therefore necessary to develop strategies that sufficiently enhance its solubility, dissolution rate and bioavailability. For this purpose, solid dispersions based on pre-selected polymers such as Eudragit® EPO, Soluplus® and Kollidon® VA 64, with 5% w/w ellagic acid loading were prepared by hot extrusion and characterized by X-ray diffraction, FTIR spectroscopy and in vitro dissolution tests in order to select the most suitable polymer for future investigations. The results showed that Eudragit® EPO was the most promising polymer for ellagic acid solid dispersions development because its extrudates allowed to obtain a solution supersaturated in ellagic acid that was stable for at least 90 min. Moreover, the resulting apparent solubility was 20 times higher than the actual solubility of ellagic acid. The extrudates also showed a high dissolution rate of ellagic acid (96.25% in 15 min), compared to the corresponding physical mixture (6.52% in 15 min) or the pure drug (1.56% in 15 min). Furthermore, increasing the loading rate of ellagic acid up to 12% in extrudates based on this polymer did not negatively influence its release profile through dissolution tests.

Keywords : Ellagic acid, Polymers, Solid dispersions, Hot melt extrusion, Solubility, Dissolution

Abbreviations : API, Active Pharmaceutical Ingredient; ASD, Amorphous Solid Dispersions; ASS, Amorphous solid solutions; CSD, crystalline solid dispersions; EA, Ellagic Acid; HME, Hot Melt Extrusion; HPMC, Hydroxypropyl Methylcellulose; PVP, Polyvinylpyrrolidone; SD, Solid Dispersions; T_{deg}, degradation temperature; T_g, glass transition temperature.

1. Introduction

Limited aqueous solubility of current active pharmaceutical ingredients (APIs) which belong to class II or IV of the Biopharmaceutical Classification System (BCS) is one of the main challenges the pharmaceutical industry faces (Göke et al., 2018; Tran and Park, 2021). The consequence of this unsatisfactory physicochemical property of the APIs is an insufficient dissolution rate, resulting in poor absorption and low bioavailability (Nyamba et al., 2021). Different approaches can be used to overcome the solubility and bioavailability issues (Anane-Adjei et al., 2022; Spoerk et al., 2022). One of these consists in incorporating the poorly soluble compounds in Solid Dispersions (SD) (Mendonsa et al., 2020). Indeed, SD might lead to particle size reduction, improved wetting, reduced agglomeration, changes in the drug physical state and disperse it on a molecular level (Asati Amit et al., 2020). Currently, there are numerous methods available for SD preparation, each of which has its advantages as well as limitations (Maha F. Emam et al., 2021). The quality of the final product is influenced by various factors, such as the basic principle involved in the method, suitability of the method, types of formulations, processing window, and practical problems involved in the process. SD preparation methods can be broadly classified into solvent-based methods and melting or fusion methods. Solvent-based methods include spray drying, electrospraying, and rotary evaporation, wherein the drug and polymer are dissolved in a solvent which is then evaporated to form SD. They are suitable for thermolabile drugs soluble in volatile solvents and the selection of the solvent system that can solubilize the drug-polymer mixture and be compatible with the formulation is the most difficult aspect of their utilization. Indeed, poor or partial solubility of the constituents may lead to longer processing times and non-homogenous SD (Iyer et al., 2021; Tran et al., 2019). While fusion methods do not require the use of organic solvents, degradation of the drug substance due to high processing temperatures is a concern. They include microwave heating, melt agglomeration, three-dimensional printing and HME. HME is one of the most efficient methods to synthesize SD (Mendonsa et al., 2020). Commonly employed in the plastics industry, the use of HME has gained favor in drug delivery applications both in academia and pharmaceutical industry (Tran et al., 2021). Indeed, it offers several advantages including the absence of solvents, less processing steps, continuous operation and great technology flexibility (Wilson et al., 2012). Thus, HME is used to manufacture various drug delivery systems such as granules, pellets, immediate and modified release tablets, implants, transdermal systems, taste- masked oral fast dissolving systems, floating drug delivery systems and ophthalmic implants (Repka et al., 2007; Thiry et al., 2017). HME can be described as the process of converting raw material into a product of uniform shape and density by forcing it through a die under defined conditions (Maniruzzaman et al., 2012). Pharmaceutical formulations by HME include the heating and softening of a mixture of drug and thermoplastic polymer, followed by the extrusion of the melt through a die into cylinders or films (Sarode et al., 2013). Other excipients such as plasticizers,

surfactants, disintegrants, salts and antioxidants can be added if required (Repka et al., 2007). Three types of SD obtained by HME are crystalline solid dispersions (CSD), amorphous solid dispersions (ASD) and amorphous solid solutions (ASS) (Janssens and Van den Mooter, 2009; Restrepo-Uribe et al., 2019). In CSD, the drug is dispersed as crystals in amorphous polymer phase (Vo et al., 2013). CSD are achieved when the thermal and mechanical energy inputs of the extruder are not sufficient to convert the crystalline form of the drug into its amorphous one. Thermographs from differential scanning calorimetry (DSC) analysis of CSD show the presence of the crystalline API melting point and the glass transition temperature (T_g) of the amorphous polymer (Shah et al., 2013). Since the drug remains in its crystalline state, CSD are very stable but less water soluble. In ASD, the drug substance is transformed into amorphous state, but it is not molecularly dispersed in the polymer matrix. Their DSC thermographs are characterized by the presence of two T_g (Tambosi et al., 2018). ASD can be unstable since the amorphous API can revert to the crystalline form. In the case of ASS, the APIs are molecularly dispersed in the polymeric matrix that exhibits a single T_g (Huang and Dai, 2014; Tambosi et al., 2018). ASS is therefore more stable and have a longer shelf life. Furthermore, the interaction forces between drug and polymer are stronger than the self-association forces among the drug molecules themselves. The crucial challenge in the development of SD is the selection of the most suitable polymer to combine with a given drug (Maha F. Emam et al., 2021; Matrose et al., 2021). Indeed, the capacity to produce the spring and parachute effect during dissolution of SD while maintaining ASD/ASS stability during storage, is strongly dependent on the polymer characteristics (Meng et al., 2015b). To identify the most suitable polymer, a variety of screening approaches can be applied (Anderson, 2018). Thus, some authors use as screening approaches, the Flory-Huggins interaction parameter, the comparison of Hansen solubility parameters (Jankovic et al., 2019), the calculation of drug- polymer mixing enthalpy (Price et al., 2019), surface free energy measurement by inverse gas chromatography (Školáková et al., 2019), melting point depression method and experimental screening of polymers for amorphous drug stabilization (Anderson, 2018; Meng et al., 2015b; Parikh et al., 2015). However, no standardized method for measuring drug-polymer solubility, miscibility and affinity with efficacy has yet been established. We are still deficient in selecting of excipients for a given drug molecule to be formulated into a stable SD (Tian et al., 2020).

Ellagic acid (EA) is a polyphenolic active compound with antimalarial and other promising therapeutic activities (Soh et al., 2009; Zazueta, 2015). EA is in class IV of the Biopharmaceutical Classification System because of its low permeability and poor water-solubility properties (Bala et al., 2005; Nyamba et al., 2021). Its estimated melting point is more than 360 °C. Being soluble neither in water nor in oils, EA belongs to the group of molecules called “brick dust”. For these drugs, the use of co-solvents, nanoparticles or SD can be interesting formulation approaches to overcome the limitations of solubility, dissolution and bioavailability (Ayad, 2015). Furthermore, different authors produced EA SD by the solvent evaporation method that significantly improved its solubility, supporting the hypothesis that the production of SD would be a promising approach for improving the solubility and oral bioavailability of EA (Yuan et al., 2021). However, to the best of our knowledge, the production of EA SD by HME has not been explored to date certainly because of its melting point estimated at more than 360 °C. In order to evaluate the potential of this approach, this first study aimed to select an appropriate polymer to use.

2. Materials and methods

2.1. MATERIALS

Ellagic acid dihydrate (98%) (Fluorochem Ltd Unit 14, Graphite Way Hadfield, Derbyshire, United Kingdom), acetonitrile HPLC grade (J.T. Baker, Deventer, The Netherlands), hydrochloric acid (37% wt. %) for analysis and monosodium phosphate (Ph. Eur, Merck, Darmstadt, Germany) were purchased. Dimethylaminoethyl methacrylate, butyl methacrylate and methyl methacrylate (Eudragit® EPO) was donated by Evonik (Darm-stadt, Germany). Polyvinyl caprolactam-polyvinyl acetate-polyethylene glycols (Soluplus®) and polyvinylpyrrolidone vinyl acetate 64 (Kollidon® VA64) were gifts from BASF (Ludwigshaven, Germany) and ultrapure water was produced by a Milli-Q system (Millipore, Bredford, MA, USA). All the other reagents and solvents were of analytical grade. The names, structures, and physicochemical properties of the polymers and drug used are given in Fig. 1.

2.2. METHODS

2.2.1. POLYMER PRE-SELECTION CRITERIA

Different criteria were established to pre-select three polymers among the most used in HME. The list of these polymers was built by J. Thiry et al in 2016 (Thiry et al., 2016). Thus, the desired polymers must have the following characteristics:

- a safety of use i.e., inert, and generally recognized as safe.
- a low hygroscopicity in order to present a good flow during extrusion process.
- a good solubility in acidic medium to present immediate release characteristics of EA.
- a glass transition (Tg) temperature between 50 and 140 °C, in order to have a favor antiplasticization of amorphous drug and an easy use during the extrusion process at reasonable temperature for pharmaceutical processes which does not exceed 180 °C.
- a degradation temperature (Tdeg) at least 100 °C higher than the Tg to avoid the risk of degradation during the extrusion process.
- a thermoplastic behavior in order to be processable in HME.

2.2.2. THERMAL CHARACTERIZATION OF RAW MATERIALS

Thermogravimetric analyses (TGA) of EA and polymers were performed using the TGA Q 500 (TA Instrument, New Castle, USA). Approximately 10 mg of raw materials were placed in small aluminum pans which were then placed on a high precision balance before being introduced into a hermetic furnace. The samples were then heated from room temperature to 500 °C at a temperature heating rate of 25 °C min^{-1}, using a nitrogen purge at 80 mL min^{-1} for EA and from room temperature to 300 °C for polymers. The weight loss of the samples as a function of temperature was recorded.

Differential scanning calorimetry (DSC) curves of polymers and EA were obtained with the Mettler-Toledo® DSC 1 (Schwerzenbach, Switzerland) controlled by STARe System software. Samples between 5.0 and 10.0 mg were accurately weighed in aluminum pans, which were crimped before testing, with

an empty crimped aluminum pan being used as the reference pan. The samples were then analyzed under a nitrogen atmosphere at a temperature heating rate of 10 °C min^{-1}. The EA analysis was initially performed from 25 °C to 400 °C. To clarify the results obtained, samples were placed in hermetically sealed aluminum pans with holes in the top, heated from 25 to 120 °C to remove moisture and then rapidly cooled to 25 °C. These samples were then heated to 520 °C to determine the melting point of EA. The polymeric samples were heated from 25 °C to 200 °C to determine the glass transition temperatures.

2.2.3. FILM CASTING

The film casting method is used to evaluate the miscibility, solubility and stability of various polymer/API blends. In this study, 20 mg of physical blends consisting of different ratios (10/90, 20/80, 30/70, 40/ 60, 50/50, and 60/40 % w/w) of EA and polymer were dissolved in a minimal volume of methanol. The solutions were then poured onto glass plates and left at room temperature for 24 h to obtain thin films after solvent evaporation. The films were then visually inspected according to literature data provided by Lang et al. (Lang et al., 2014). Blank samples consisting of EA or polymer were also made for comparison.

2.2.4. MANUFACTURE OF SOLID DISPERSIONS

EA SD were prepared by hot melt extrusion, using an 18 mm twin screw hot melt extruder (L/D = 24, Scamex1, Crosne, France) with a standard screw configuration containing 2 kneading zones and a 2 mm die. Physical mixtures (50 g) consisting of 5% w/w EA and 95% polymer were homogenized for 20 min with a Turbula1 shaker-mixer (Clifton, USA). The mixtures were then loaded into the volumetric feeder of the extruder which fed the barrel through two screws rotating at 1 rpm. The extruder screws speed was set at 25 rpm and the temperature gradient applied to the 5 heating zones of the barrel was based on the polymer used. These temperatures were 155 °C, 160 °C, 165 °C, 170 °C and 175 °C for Soluplus®, 160 °C, 165 °C, 170 °C, 175 °C and 180 °C for Eudragit® EPO and Kollidon® VA64.

2.2.5. DETERMINATION OF DRUG CONTENT

To determine the percentage of EA in the extrudates, samples equivalent to 1 mg EA were accurately weighed from the milled extrudates and dissolved in methanol. The concentration of EA in the resulting solutions was determined by high-performance liquid chromatography (HPLC), using an Agilent 1100 HPLC system (Agilent Technologies, Santa Clara, CA). Chromatographic separation was performed using a LiChrospher®100 RP-18 column (125x4 mm, 5 µm) at a temperature of 40.0 °C. The mobile phase flow rate consisting of phosphate buffer pH 2.5 and acetonitrile (75:25 v/v), was kept constant at 1.0 mL/min. The injection volume was 50 µL, the total analysis time was 6 min, and EA was detected at the wavelength of 254 nm. The results were analyzed using Agilent OpenLAB Control Panel software. The percentage EA content was calculated relative to the theoretical mass of EA dissolved in methanol.

2.2.6. IN VITRO NON SINK DISSOLUTION TESTING

In order to use samples with comparable particle sizes, the extrudates were milled using a commercial grinder (Frewitt FreDrive-Lab HammerWitt-Lab, Granges-Paccot, Switzerland) and then passed

through a sieve with mesh openings of 0.35 um. The milled extrudates, physical mixtures and pure EA were manually encapsulated into a size 0 colorless gelatin capsule, containing 2 mg of the drug. This amount allowed the conduction of the dissolution tests under non-sink conditions in order to obtain a potential supersaturation of EA in the dissolution medium. Dissolution was performed using the Sotax® AT7 (Sotax, The Netherlands) USPII paddle method apparatus. The stirring speed was 100 rpm, the temperature was maintained at 37 ± 0.5 °C and the medium was 1000 mL of 0.1 N HCl. A volume of 2 mL was sampled and replaced with fresh media at intervals of 5 min, 15 min, 30 min, 45 min, 60 min, 75 min and 90 min, filtered on a Millex-HV Durapore® PVDF filter (0.45 μm, 13 mm diameter) before being analyzed by HPLC as described above. The dissolution profiles of EA from the milled extrudates were compared to those from the physical mixture and the pure drug, using two-way ANOVA tests.

2.2.7. X-RAY POWDER DIFFRACTION (XRPD)

To evaluate the crystallinity, X-ray diffractograms of raw material (EA and polymers) and the different milled extrudates were collected, using a Bruker D8 TWIN-TWIN diffractometer in Bragg-Brentano configuration (Cu Kalpha radiation, variable divergence slit V6, sample rotation 15 rpm) with a Lynxeye XET detector in 1D mode (192 channels) and a total scan time of 15 min or 40 min for a 0.02° step size.

2.2.8. FOURIER TRANSFORMS INFRARED SPECTROSCOPY (FTIR)

Mid-infrared spectra of EA, polymeric carriers, physical mixtures, as well as extrudates, were performed using a Frontier FT-IR spectrophotometer (Perkin Elmer, Waltham, USA) equipped with a diamond crystal ATR device and a DTGS detector. Measurements were made at room temperature on the samples directly placed on the ATR and the scanning range of 4000 to 650 cm^{-1}. The FT-IR spectra of the extrudates were then compared with those of pure EA, polymers and physical mixtures.

2.2.9. EA AQUEOUS SOLUBILITY DETERMINATION

An excess amount of EA (1 mg) was put in 10 mL of miliQ water or HCL 0.1 N. The resulting suspensions were stirred at 37 °C for 24 h using a shaking bath at a speed of 140 rpm and then filtered on a Millex-HV Durapore® PVDF filter (0.45 μm, 13 mm diameter) before being analyzed by HPLC.

2.2.10. DRUG LOADING ENHANCEMENT

To determine the ideal drug loading in the most promising polymer i.e. Eudragit® EPO, SD with increasing amounts of EA (7.5%, 10% and 12% w/w) were prepared. The screw speed of the extruder was adjusted to 100 rpm and the feed rate was set at 4 rpm. The screw configuration as well as the applied temperature gradient were the same as those used previously (section 2.2.3).

2.2.11. STATISTICAL ANALYSIS

The data statistics were performed using Graphpad Prism version 5.03 software (GraphPad Software, Inc., La Jolla, CA, USA) by two-way ANOVA test and Tuckey tests. The results are presented as mean ± SD. Statistical differences were considered significant between the groups if the p-value was < 0.05. All experiments were carried out in triplicate ($n = 3$).

3. Results and discussion

3.1. PRE-SELECTION OF POLYMERS

The application of the required ideal characteristics to the list of the common polymers used in HME (Thiry et al, 2016) has allowed to retain five polymers, Eudragit® EPO, Soluplus®, Kollidon® VA 64, Kollidon® 12 PF (PVP) and Affinisol® (HPMC). Kollidon® 12 PF and Affinisol® HPMC were then dismissed. In a previous study, Bin Li et al demonstrated that PVP was not a practical candidate for EA SD. Indeed, while EA and PVP -based SD, produced by solvent evaporation during their study, increased the solubility of EA more than 45-fold, EA recrystallized very rapidly from supersaturated EA solutions formed by these SD (Li et al., 2013). This instability is one of the main drawbacks of SD as it may negate the advantages of these forms in terms of improved solubility and bioavailability compared to pure drug. It occurs when drug-polymer interactions are not sufficient to delay nucleation and/or crystal growth of the API (Kong et al., 2023). Therefore, Bin Li et al. recommended the cellulose derivatives, particularly hydroxypropyl methylcellulose acetate succinate (HPMCAS) to improve the solubility and stability of EA. However, this polymer being soluble in water at pH higher than 5.5, it is not a good candidate for the production of EA-based immediate release forms (Sarode et al., 2014). Yuan et al. also produced by solvent evaporation method EA and PVP-based SD that increased the solubility of EA by more than 20 times. However, these authors did not evaluate the ability of these SD to form and maintain supersaturated EA solutions (Yuan et al., 2021). Affinisol® (HPMC) is much more used as an excipient for the production of modified release forms by HME (Zhang et al., 2017). Furthermore, extrusion tests carried out by our research group with physical mixtures containing 5% EA and 95% (w/w) Affinisol® (HPMC), resulted in increases in extruder torque up to 40 Nm, blocking the screws. Eudragit® EPO, the first of the three selected polymers, is a copolymer of methyl methacrylate (25%), butyl methacrylate (25%) and dimethylamino ethylmethacrylate (50%). The carbonyl groups act as proton acceptors and are able to interact with proton donating groups. In addition, the nitrogen of the dimethylamino group is a strong base, making Eudragit® EPO a pH-dependent solubility polymer (Liu et al., 2010). Thus, at neutral pH values, Eudragit® EPO is insoluble since the basic dimethylamino groups are unionized (Salmani et al., 2015). On the contrary, at acidic pH values as the gastric medium, these groups are ionized, resulting in rapid dissolution of the polymer (Gallardo et al., 2008). Eudragit® EPO, widely reported as a hot-melt extrusion polymeric carrier, is therefore able to interact by ionic bonds of cation/anion type with weak acids like EA (J. Li et al., 2015), although this type of interaction has not been demonstrated. Soluplus® is an amphiphilic polymer exclusively synthesized for HME. It enhances apparent solubility by the formation of micellar structures and non- covalent interactions with the drug molecules. Kollidon® VA 64 is a semi-crystalline amphiphilic polymer. Due to its amide structure, it provides APIs with hydrogen bond acceptors groups. It is therefore a suitable carrier for a wide variety of drug (Patel and Serajuddin, 2022).

3.2. THERMAL ANALYSIS OF RAW MATERIALS

The thermal analysis method is an indispensable and well established routine tool for the characterization of SD as well as the raw materials entering in their composition. TGA and DSC are two

of the most popular techniques (Liu et al., 2018). In order to define the temperature window in hot-melt extrusion to avoid thermal degradation, TGA was used to evaluate the thermal stability of EA and polymers. As illustrated in Fig. 2, EA was thermally stable up to 471 °C, although 2 % water related to EA was lost at temperatures below 120 °C. EA then, gradually decomposes from this temperature and the decomposition is complete at 493 °C. This result is close to that of Hussein et al. who found that EA decomposed at 496 °C (Hussein et al., 2011). In another study, Y. Li et al. found strong decomposition (82% weight loss) of pure EA at 635 °C (Y. Li et al., 2015). Similar results were also reported by Mirulanini et al. (Arulmozhi et al., 2013). Avachat et al. found a single endothermic peak at 302.78 °C in the thermogram of EA and interpreted it as its degradation temperature (Avachat and Patel, 2015). The data on the thermal behavior of EA remain heterogeneous, the only common point being its stability at high temperatures. The degradation temperatures of the polymers (Fig. 1) were 230 °C, 250 °C and 278 °C for Kollidon® VA 64, Eudragit® EPO and Soluplus® respectively. Therefore, the use of 180 °C (at least 50 °C below the T_{deg}) as the maximum extrusion temperature should present a minimal risk of thermal degradation for our raw materials during the process.

DSC is the most common thermal analysis technique used for a wide range of applications, including fundamental research, development of new materials and quality inspection in industrial production (Zheng et al., 2019). In this technique, the energy input associated with heating materials can be measured to detect thermal transitions such as the melting point, glass transition, polymorphic form transformation and recrystallization (Liu et al., 2018). The characterization of EA by DSC in this study, was carried out in three steps. The first step carried out on a temperature range of 25 to 400 °C, showed a thermogram with an endothermic peak at 112 °C probably related to the evaporation of the water contained in the sample as already observed by Hussein et al. in 2011 (Hussein et al., 2011) and Li et al. in 2021 (Li et al., 2021). Furthermore, Dávalos et al. found no significant change in the DSC ´ thermogram of anhydrous EA in the measurement range from −10 °C to 476 °C (Dávalos et al., 2019). However, the DSC thermogram obtained by Yuan et al. showed a sharp endothermic peak of around 154.6 °C, attributed by them as melting process (Yuan et al., 2021). These authors did not rule out the possibility of an endothermic peak related to water evaporation since their EA standard had a purity of 97%. The second step was performed at a temperature range of 25 to 120 °C in order to remove the moisture contained in the sample. The third step aimed at the determination of the melting point of EA was spread over a temperature range from 25 to 520 °C. As illustrated in Fig. 3, the DSC thermogram does not show significant changes until the degradation of the EA around 490 °C materialized by an endothermic peak. Therefore, the melting temperature of the EA has not been obtained. Bin Li et al. 2013 made the same observation and explained it by the degradation of EA at 360 °C (Li et al., 2013). Indeed, many drugs are heat-sensitive, degrading upon or even before melting (Guo et al., 2014; Haser et al., 2017). DSC may be the most widely used method in SD characterization. However, because of this particular thermal behavior of EA, we opted for the use of XRPD to characterize the physical state of EA in our extrudates. The thermal characteristics of the three polymers such as Tg are depicted in the Fig. 1.

3.3. FILM CASTING

Film casting technique in which the active substance and the polymer are solubilized in an organic solvent to generate uniform thickness films (Psimadas et al., 2012), was used to determine the solubilization capacity of EA by each preselected polymer. This technique is widely used to discard incompatible API-polymer excipient pairs because after film preparation, API stability and recrystallization can be assessed by thermal methods like DSC (Meng et al., 2015a). However, for molecules like EA with very high melting points (estimated to be over 360 °C), well above the degradation temperature of all the polymers used in this study, the use of DSC to characterize the physical state of EA in films would require the application of high temperatures with the risk of polymers degradation. The thin EA/polymer films obtained have been therefore visually inspected and according to the literature (Lang et al., 2014), the transparent and opaque films have been considered as amorphous and crystalline solid dispersions, respectively. Thus, films of Eudragit® EPO were amorphous up to 20 % EA, those of Soluplus® up to 30% and those of Kollidon® VA 64 were crystalline at 10% EA.

3.4. EA AQUEOUS SOLUBILITY STUDIES

The solubilities at 37 °C of EA in HCl 0.1 N and in purified water were 0.1 ± 0.01 µg/mL and 1.48 ± 0.37 µg/mL, respectively. Because of its acidic nature, the solubility of EA in acid medium is lower than the one in water (Bala et al., 2006). The samples were measured without any special treatment preventing precipitation during cooling to room temperature. However, no precipitates were detected by visual inspection that was performed on all samples prior measurement. The aqueous solubility is close to what was observed by Y. Li et al. (1.8 ± 0.90 µg/mL) (Y. Li et al., 2015) but very lower than that of Bala et al (9.7 µg/mL). This disparity in results could be explained by methodological differences. Indeed, the method used by Bala et al. consisted in sonicating the samples for 10 min before maintaining them at 37 °C in shaking water for five days. Aliquots were then withdrawn every 24 h, centrifuged, diluted in phosphate buffer at pH 7.4 and the concentration of EA determined by UV absorbance. Equilibrium was reached within five day. Sonication, analysis time and the use of phosphate buffer at pH 7.4 to dilute the samples could have contributed to achieve higher solubility in their study.

3.5. MANUFACTURING OF SOLID DISPERSIONS BY HOT MELT EXTRUSION

During hot melt extrusion, thermal and mechanical energy from heated barrels and rotating screws is applied to the drug and polymer blend resulting in a SD (Alsulays et al., 2015). The physical aspects of SD depend on the physicochemical properties of the carrier and the drug, the drug-carrier interactions and the preparation method (Liu et al., 2013). Furthermore, they orientate on the amorphous or crystalline character of SD (Shah et al., 2013). The extrudates obtained from EA and the three selected polymers were opaque (Fig. 4) evoking crystalline SD (CSD) rather than amorphous SD (ASD). Indeed, to obtain ASD by HME, API must either melt or solubilize in the molten polymers during the extrusion process (Moseson et al., 2020) which is typically performed at 20 °C above the melting point of the drug (Haser et al., 2017). For EA, this temperature is greater than 380 °C, which is well above the degradation temperature of the polymers used in this study. Therefore, treatment of EA at a maximum

of 180 °C by HME could lead to its amorphization if the polymer used sufficiently depressed its melting temperature and/or if the shear induced by the screw speed was adequate (Haser et al., 2017). For example, Tian et al. showed that processing APIs below their melting point for an ASD was possible where there was high miscibility between the drug and the polymer (Tian et al., 2020). Furthermore, Hughey et al., 2011 found that Kollidon® VA 64 had the ability to suppress the melting point of meloxicam from 275 °C to 175 °C (Hughey et al., 2011).

Although the non-amorphization of the API, its apparent solubility and dissolution rate from CSD produced by HME can be significantly enhanced by parameters such as reducing drug particle size, increasing drug wettability and forming soluble drug-carrier complexes (Li et al., 2020). Thus, CSD were designed to improve the dissolution of three poorly water-soluble drugs with high melting point like griseofulvin (10% and 50%), spironolactone (10%) and phenytoin (10%) in mannitol (Shah et al., 2013). Moreover, the presence of crystallinity doesn't raise the problem of physical stability compared to amorphous one (Thommes et al., 2011).

3.6. CHARACTERISTICS OF THE SOLID DISPERSIONS

3.6.1. DRUG CONTENT

The EA content in the extrudates was evaluated by HPLC and ranged from 89.86 ± 1.15 % to 98.71 ± 2.06 % of its theoretical amount. Whatever the polymer used, it ranged from 97.71 ± 1.34 % to 98.71 ± 2.06 % and 89.86 ± 1.15 % to 90.60 ± 1.27 % for the extrudates obtained with a screw speed of 25 rpm (extrudates with 5% w/w EA loading) and 100 rpm (extrudates with 7.5, 10 and 12 % w/w EA loading) respectively. The slight loss of API observed during the HME process with a screw speed of 25 rpm could be explained by the equipment surface adherence. In fact, the EA is a fine powder that could adhere to the feeder screws during the process. The EA loss is more significant when the screw speed increases from 25 rpm to 100 during the HME process. This could be explained by the degradation of the drug due to the increase of the material temperature (+20 °C) during the extrusion process. Indeed, it is well known that an increase in screw speed leads to high shear, a rise in material temperature and an increased risk of drug degradation due to the increased mechanical energy (Ghosh et al., 2012; Reitz et al., 2013).

3.6.2. X-RAY POWDER DIFFRACTION (XRPD)

The X-ray diffraction spectra of raw materials (A) and extrudates (B) are presented in Fig. 5. EA showed peaks at 2 theta of 20.90°, 25.14°, 26.43°, 28.30° and 29.29°. With Eudragit® EPO extrudates, the EA peak at 25.85° appeared at 25.14° and the most intense peak observed at 28.30° was absent, probably due to a huge decrease of the EA crystallinity. However, this intense peak was present in the spectra of Soluplus® and Kollidon® VA64 extrudates, confirming the presence of residual EA crystals. As the above visual observations, the X-ray diffraction results confirm that EA, a high melting point drug, was not completely amorphized during the extrusion process. The presence of the residual crystals proves the inability of the process parameters and polymers to amorphize all of the EA with an extrusion temperature of 180 °C (Huang et al., 2019; LaFountaine et al., 2016).

3.6.3. FOURIER TRANSFORMS INFRARED SPECTROSCOPY (FTIR)

FT-IR analysis was performed to identify chemical or physical interactions between EA and the different polymeric carriers. FT-IR spectra of pure drug, polymers, and physical mixtures and SD samples are presented in Fig. 6 (A, B and C). The spectra of EA, Eudragit® EPO, their physical mixture, and extrudates are shown in Fig. 6 A. Pure EA showed six characteristic bands between 4000 and 1500 cm^{-1}. The first two bands (at 3474 cm^{-1} and 3151 cm^{-1}) and the third one (at 1717 cm^{-1}) correspond to the valence vibrations of the hydroxyl (O–H) and ketone (C = O) groups, respectively. The last three bands at 1615, 1582 and 1507 cm^{-1} correspond to the C = C bond of the aromatic ring. In the fingerprint region between 1500 and 650 cm^{-1}, several bands were also present. The bands at 1448 and 1398 cm^{-1} correspond to the C–H bond deformation vibrations and those at 1324 and 1033 cm^{-1} are the symmetric and asymmetric vibrations of the C-O bond. The band at 1189, 1109 and 753 cm^{-1} are respectively the vibration of the phenolic C-O bond, the C–C bond, and a substituted aromatic ring at position 4. These results are similar to those of Savic et al (Savic et al., 2019). The FT-IR spectrum of Eudragit® EPO showed a strong band at 1722 cm^{-1}, corresponding to the valence vibrations of the carboxyl groups of the three monomers. The bands at 2951 and 2875 cm^{-1} are attributed to asymmetric and symmetric CH_3 groups, those at 2822 and 2767 cm^{-1} to the dimethylamino groups and the one at 1447 cm^{-1} to the C–H bending vibration for the methyl group. The bands at 1270 and 1238 cm^{-1} are due to the C-O stretching vibration of the ester group and the one at 1153 cm^{-1} is attributed to the C-N stretching absorption of the aliphatic amines and/or the C-O stretching vibration of the ester groups. These observations are close to the previous ones made by other authors (Juppo et al., 2003; Menjoge and Kulkarni, 2007). The FTIR spectrum of EA/ Eudragit® EPO extrudates is close to that of pure Eudragit® EPO. The presence of EA is materialized by specific bands, notably those at 1582, 1356 and 817 cm^{-1}. However, the bands of the O–H group of EA at 3474 and 3135 cm^{-1} were absent, probably due to their involvement in the interaction with Eudragit® EPO. Indeed, the band of the EPO carboxyl groups showed a broadening and a slight decrease in intensity, suggesting the formation of H-bonds between the Eudragit® EPO carbonyl groups that accept H atoms from the OH groups of EA. Li et al. have demonstrated the same type of interaction between Eudragit® EPO and curcumin, another poorly water-soluble weak acid (J. Li et al., 2015). The spectrum of the physical mixture of EA with Eudragit® EPO showed characteristic peaks of these two substances. However, a significant decrease of the intensity of EA specific peaks is observed, suggesting some interactions between the two substances. The FT-IR spectra of EA, Soluplus®, their physical mixture, and extrudates are shown in Fig. 6 B. A broad band at 3463 cm-1 corresponding to the valence vibrations of free hydroxyl groups (O–H) and stretching bands of asymmetric and symmetric CH groups are present at 2927 and 2865 cm^{-1}. The valence vibration band of C = O esters, C = O tertiary amides and C- O-C group stretching appear at 1733, 1631 and 1480 cm^{-1} respectively. The spectrum of Soluplus® / EA extrudates shows a broadening of the band at 3463 cm^{-1}, masking the bands specific of EA OH groups. In addition, the C = O ester and C = O tertiary amides bands of Soluplus® now appear at 1828 cm^{-1} instead of 1733 cm^{-1} and at 1652 cm^{-1} instead of 1631 cm^{-1}, suggesting interactions between these groups with OH of EA. Similar results were also observed in previous works (Shamma and Basha, 2013) (Djuris et al., 2013). In the physical mixture, only a simple superposition of the spectra is observed, suggesting only limited interactions. The FTIR spectra of EA, Kollidon® VA64, their physical mixture, and extrudates are shown in Fig. 6 C.

Kollidon® VA64 contains two hydrogen bonding receptor groups, derived from the C = O group of the pyrrolidone ring with a vibrational band at 1669 cm^{-1} and from vinyl acetate with a vibrational band at 1733 cm^{-1}. The FTIR spectra of the physical mixtures and extrudates shows a simple superposition of the individual spectra, indicating limited interaction between EA and Kollidon® VA64. However, there are changes in the intensity and position of the bands of the OH moieties of EA and those of the two hydrogen bonding receptor groups of Kollidon® VA64.

3.6.4. IN VITRO NON-SINK DISSOLUTION TESTING

In vitro dissolution testing plays an important role in drug formulation development and quality control because it may be relevant to the prediction of *in vivo* performance (Grignard et al., 2017; Markopoulos et al., 2015). The results of the dissolution tests, intentionally performed under non-sink conditions, are presented in Fig. 7. The EA release was much faster from all the extrudates than that from the physical mixtures or pure EA powder. The dissolution rates obtained at 15 min with Soluplus® extrudates, Soluplus® physical mixture and pure drug were 42.5 ± 0.70%, 9 ± 0.30%, and 1.56 ± 0.16%, respectively. The maximum rate of EA dissolution from the extrudates depended on the polymers used. It was 41.50 ± 4.23 %, 54 ± 0.74 % and 99.61 ± 1.06 % with Kollidon® VA64, Soluplus® and Eudragit® EPO respectively. Thus, the increase in apparent solubility of EA resulting from these dissolution rates was 8.2, 10.8 and 19.92 times its actual solubility. Finally, the EA release profiles from the extrudates were different from one polymer to another, confirming the complexity of using polymeric matrices to accelerate the release of poorly soluble API (Shadambikar et al., 2020). With Kollidon® VA64 extrudates, the EA release reached 41.50 ± 4.23 % at 15 min and suddenly dropped, probably due to a recrystallization resulting in the incapacity of this polymer to stabilize EA at supersaturated concentration. This phenomenon occurs when the “parachute” effect of the polymer to maintain the supersaturation fails. Polymeric excipients that increase the drug aqueous solubility can decrease the free drug available for nuclei/ seed formation and thus, delay the nucleation. Stabilization can be effective when the drug concentration in the polymer matrix is lower than its solubility. In this case, the mixture is in an equilibrium state that preserves it from any unmixing process (Rumondor et al., 2009). In the opposite case like EA - Kollidon® VA64 extrudates, it is apparent and the recrystallization of the API can occur. The dissolution rate of the physical mixture and pure product were 12.28 ± 3.18% and 1.56 ± 0.16% respectively.

On the contrary to Kollidon, the dissolution of EA from Soluplus® extrudates progressively increased over time, reaching 42.5 ± 0.70% and 54 ± 0.74% at 15 min and 90 min respectively. The supersaturated solutions of EA were thus more stable with Soluplus®, a polymeric solubilizer consists of 13 % polyethylene glycol 6000, 57% polyvinylcaprolactam and 30% polyvinyl acetate. As already observed by some authors (Hughey et al., 2013; Thiry et al., 2016), this structure leads to the formation of a gel in aqueous media, which slows down the release of the API. These authors also recommend the use of sodium bicarbonate to decrease the gel effect of this polymer. Higuchi et al., have shown that formulating the drug as a SD changes the dissolution behavior, whereby the dissolution rate of each component depends on the composition and interactions. This result was then further investigated and it is accepted that at high drug loadings, the polymer dissolves faster than the drug. In this case, the drug release is slow and incongruent. At low drug loadings on the other hand, the drug dissolution

rate is dependent on the polymer dissolution rate. The drug release is therefore congruent. It is fast if the polymer dissolves quickly and slow if the polymer dissolves slowly (Saboo et al., 2020,). Thus, the incomplete dissolution rate of EA from the Soluplus® extrudates with 5% w/w EA loading, could be explained by the dissolution behavior of the polymer. Indeed, in addition to the gelling effect of Soluplus® which may negatively impact the rate and extent of drug release, extrudate particles were present in the dissolution media at the end of the tests. Used as a matrix polymer, as a solubilizer through micelle formation in water and as a carrier in SD formation, Soluplus® has a high molecular weight (118000 g/mol) slowing down its solubilization and consequently that of the drugs contained in its SD at low loading rates (Guan et al., 2019). Another factor that could explain the incomplete dissolution rate of Soluplus® extrudates could be the presence of crystalline residues revealed by XRPD. Indeed, these residues dissolve much more slowly than the amorphous forms (Kanaujia et al., 2015).

Compared to Soluplus® and Kollidon® VA64, Eudragit® EPO appears to be the most promising polymer with regard to the improving of the EA solubility and bioavailability. Indeed, the EA release from Eudragit® EPO extrudates was the most rapid and complete ($p < 0.05$) (96.25 ± 5.30 % and 99.61 ± 1.06 % at 15 and 90 min). This stability of drug in the supersaturated state indicates a good interaction between this polymer and EA. Eudragit® EPO being a cationic polymer, it is capable to establish cation/anion bonds in solution with weak acids like EA (J. Li et al., 2015). However, this eventuality remains unlikely in the present study because in acid medium, the weak acids are in a non- ionized form. The formation of hydrogen bonds between EA hydroxyls as the donor and the oxygen atoms in the methacrylate backbone of Eudragit® EPO as the acceptor, is the more probable interactions, as suggested by the FT-IR results (Fig. 6**)** and the case with atorvastatin (Salmani et al., 2015).

3.7. EFFECT OF INCREASING DRUG LOAD ON EXTRUDATES CHARACTERISTICS

It seems well established that drug load has a direct impact on dissolution and subsequently on the properties of the dissolved SD (Gottschalk et al., 2022). Indeed, an increase of the drug proportion leads to a decrease in that of the polymer, which can have a negative impact on the dissolution rate and the stability of the dissolved product (Shi et al., 2022). However, the low loaded polymer matrices are only suitable for delivering low dose drugs (Hou et al., 2017). In fact, a low drug loading may result in a high pill burden for the patient, arising from a large dosage form or multiple dosage units, hence the need to find the optimum loading rate (Luebbert et al., 2017). In general, the drug loading range of SD is often set between 10 and 30 % w/w with 25 % w/ w being the target drug loading and drug loadings exceeding these i.e., up to 50 % are generally seen as the exception to the rule. However, during preclinical development, optimum drug loading must be investigated on a case-by-case basis. OMARIA® (Orissa Malaria Research Indigenous Attempt) is a pharmaceutical preparation used in India for the treatment of malaria at a dose of 1 capsule/8h for 3 days or 1 capsule/day in prophylaxis for 2 weeks. Each capsule contains 825–850 mg of sun-dried rinds from the immature fruits of pomegranate (*Punica granatum*) including 13.5 % of EA (111.38–114.75 mg) (Dell'Agli et al., 2009). For such therapeutic use, 6683.8–6885 mg of extrudates with 5% w/w EA loading will be required per day, which may require several capsules per administration and could reduce patient compliance. Therefore, we

investigated using Eudragit® EPO, the most suitable polymer, the effect of increasing the loading rate of EA on its dissolution profile and on the X-ray diffractograms of the extrudates.

Thus, physical mixtures of EA and Eudragit® EPO at 7.5/92.5%, 10/ 90% and 12/88% w/w have been successfully extruded with a torque varying between 20Nm and 40Nm. Higher load of EA has not been extruded because it required a torque higher than 40 Nm, the maximum usable with the extruder. As can be observed in Fig. 8, any significantly decrease of the EA dissolution rate was observed with the different extrudates. The extrudability of the physical blends therefore remains the main limiting factor. The use of plasticizer could be an interesting approach to meet this challenge. The results of the characterization of the extrudates by X-ray diffraction are presented in Fig. 9**.** As the diffractogram of the extrudates with 5% w/w EA loading, that of the extrudates with 7.5% w/w does not show the main EA peak at 28.30°, which may be due to the significant dissolution of EA in the polymer melt during extrusion. This peak, on the other hand, is present in extrudates with higher EA content, probably due to undissolved crystal residues.

4. Conclusion

This study aimed to select the more suitable polymer to be used for preparing by HME EA SD. Based on the polymer properties compatible with HME process, three polymers (Eudragit® EPO, Kollidon®VA 64 and Soluplus®) have been retained and investigated. The X-Ray diffraction analysis has shown that the solid dispersions (SD) with 5% w/w EA loading produced by HME all contained residual crystalline drug. However, the drug release profiles from the three various polymeric extrudates were dissimilar. While EA release from the Kollidon® VA64 extrudates recrystallize very quickly, that from Soluplus® is progressive and incomplete for 90 min and that of Eudragit® EPO is rapid, complete, without any recrystallization. Eudragit® EPO, which is extrudable up to 12% w/w EA loading while maintaining a better dissolution profile, appears to be the most suitable polymer for the development of EA solid dispersions by HME.

CRediT authorship contribution statement

Isaïe Nyamba: Investigation, Visualization, Methodology, Writing – original draft. **Olivier Jennotte:** Writing – review & editing. **Charles B. Sombié:** Writing – review & editing. **Anna Lechanteur:** Validation, Supervision, Writing – review & editing. **Pierre-Yves Sacre:** Writing – review & editing. **Abdoulaye Djandé:** Writing – review & editing. **Rasmané Semdé:** Validation, Supervision, Writing – review & editing. **Brigitte Evrard:** Validation, Supervision, Writing – review & editing.

Declaration of Competing Interest

The authors declare that they have no known competing financial interests or personal relationships that could have appeared to influence the work reported in this paper.

Data availability

No data was used for the research described in the article.

Acknowledgments

Authors would like to acknowledge the Academy for research and Higher Education- Development Cooperation Committee (ARES-CCD) for the financial support.

Figures

Fig. 1. *Names, structures and physicochemical properties of polymers and ellagic acid used in this study.*

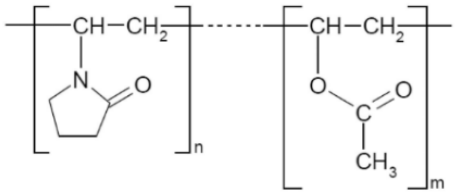

Kollidon® VA 64 (polyvinylpyrrolidone vinyl acetate copolymer (60/40))

$T_g \approx 106°C$ Molar weight ≈ 45,000 g/mol

$T_{deg} \approx 230°C$ (Patel and Serajuddin, 2022)

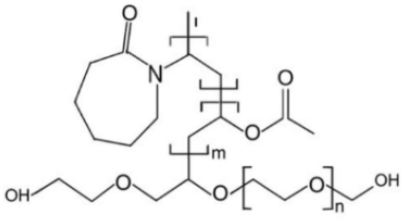

Soluplus® (Polyvinyl caprolactam–polyvinyl acetate– polyethyleneglycol Copolymer (57/30/13)

$T_g \approx 60°C$ Molar weight ≈ 118000 g/mol

$T_{deg} \approx 278°C$ (Lamichhane et al., 2022)

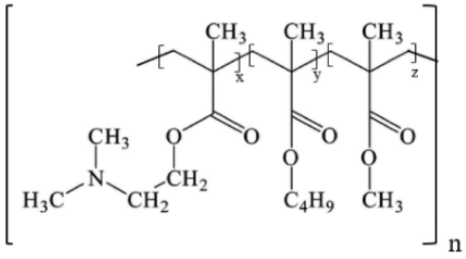

Eudragit® EPO (dimethylaminoethyl methacrylate–butylmethacrylate–methylmethacrylate copolymer (50/25/25))

$T_g \approx 55°C$ Molar weight ≈ 47000 g/mol

$T_{deg} \approx 250°C$ (Psimadas et al., 2012)

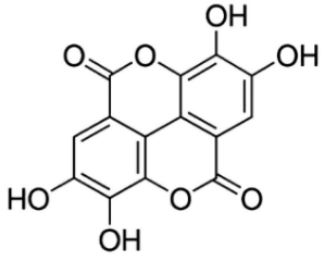

Ellagic acid (3,7,8-tetrahydroxy-chromeno [5,4,3-cde]-chromene-5,10-dione

Molar weight: 302.197 g/mol (Zazueta, 2015)

Fig. 2. *Thermogram of ellagic acid (EA) obtained by thermogravimetric analysis (TGA) from room temperature to 500 °C (speed: 25 °C/min).*

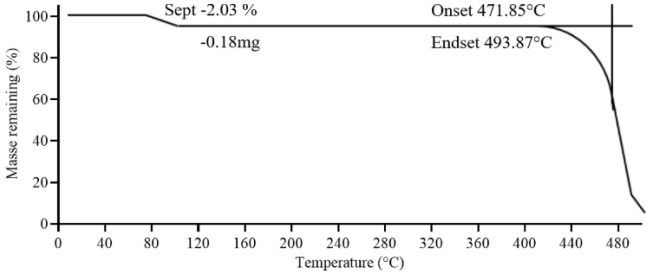

Fig. 3. *Thermogram of ellagic acid (EA) obtained by Differential scanning calorimetry (DSC) from 25 °C To 520 °C (speed: 10 °C/min).*

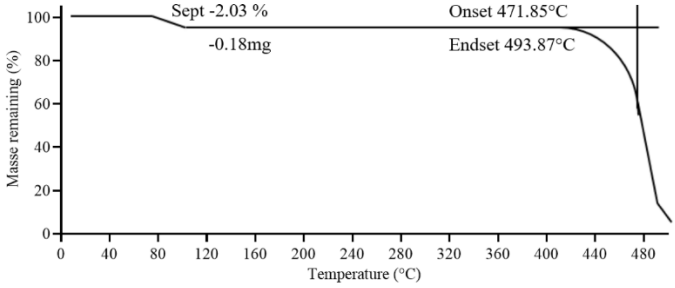

Fig. 4. *Pictures of extrudates composed of EA/polymers (5/95 % w/w), obtained by HME. Picture 5X5cm2, 674X189 pixels taken with a digital camera. Extrudates of EA/Kollidon® VA64 (A), EA/Soluplus® (B) and EA/Eudragit® EPO (C).*

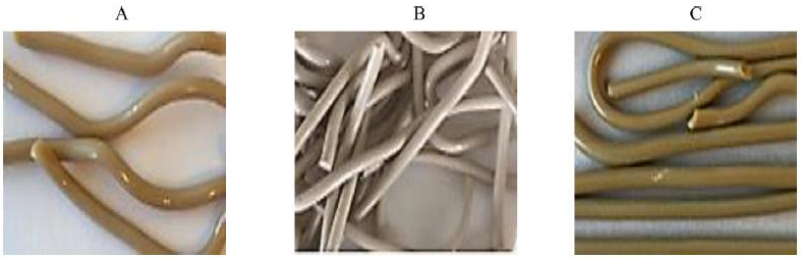

Fig. 5. *XRPD diffractograms of ellagic acid (EA), Eudragit® EPO (EPO), Soluplus® (SOL) and Kollidon® VA64 (KOL) (A); EA and milled extrudates composed of EA/ polymer (5/95% w/w) produced by HME (B).*

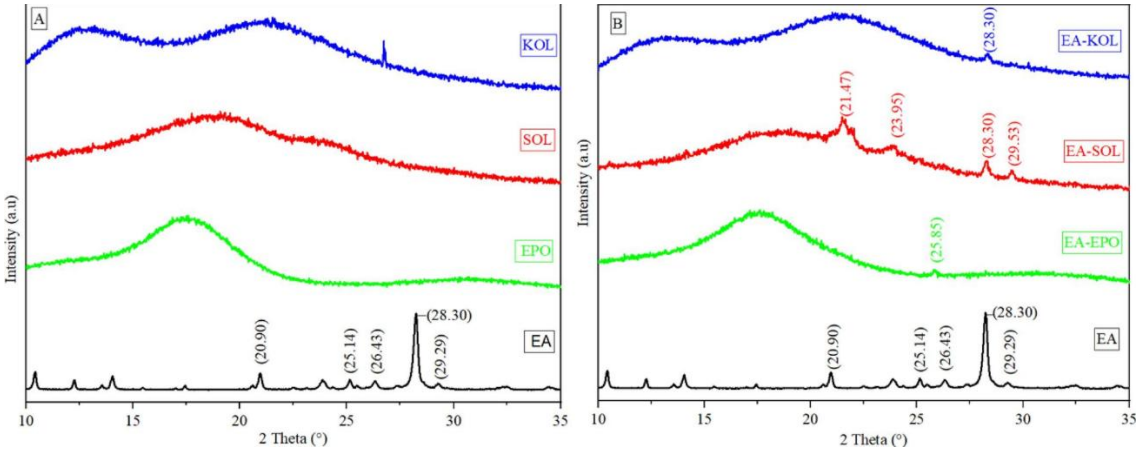

Fig. 6. *FTIR spectra of ellagic acid (black), Eudragit® EPO (blue), milled extrudates (green) and physical mixture (red) composed of ellagic acid / Eudragit® EPO (5/ 95% w/w) (A); FTIR spectra of ellagic acid (black), Soluplus® (blue), milled extrudates (green) and physical mixture (red) composed of ellagic acid / Soluplus® (5/ 95% w/w) (B) and FTIR spectra of ellagic acid (black), Kollidon® VA64 (blue), milled extrudates (green) and physical mixture (red) composed of ellagic acid / Kollidon® VA64 (5/95% w/w) (C). (For interpretation of the references to colour in this figure legend, the reader is referred to the web version of this article.)*

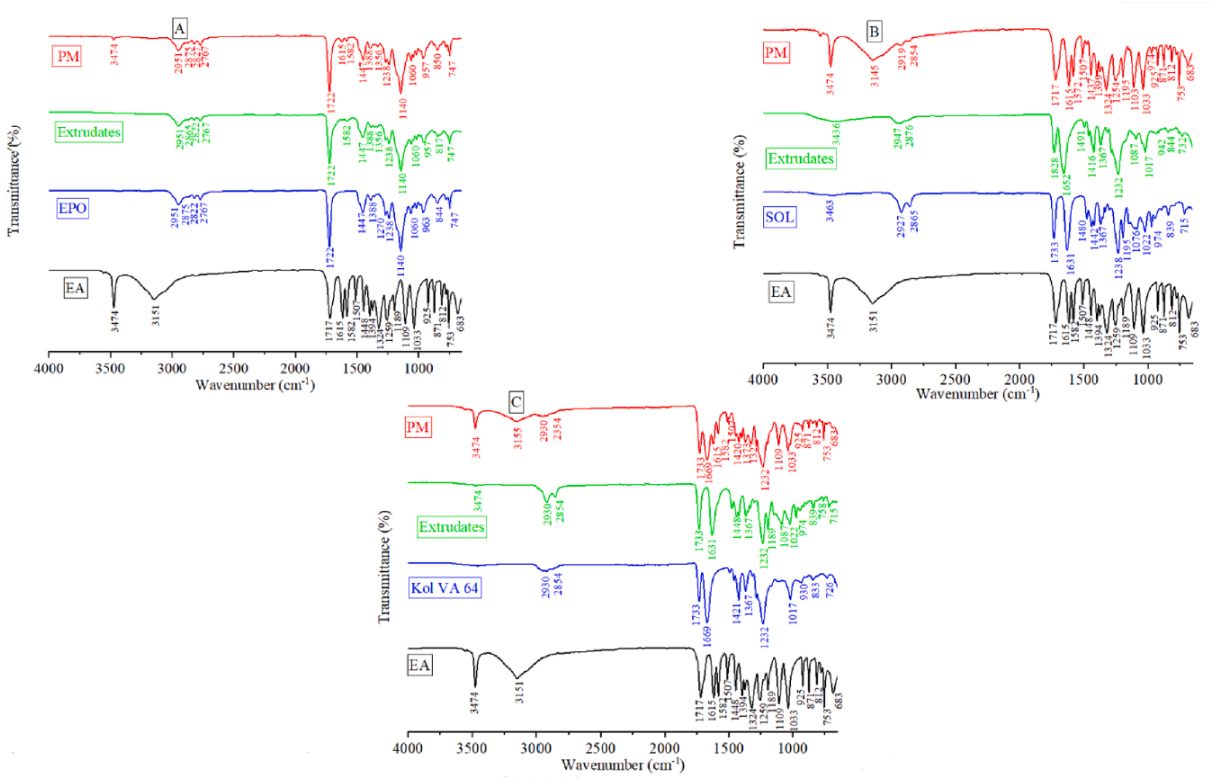

Fig. 7. *Drug dissolution profiles from physical mixtures composed of ellagic acid /polymer (5/95% w/w) (dotted lines) and from pure ellagic acid and milled extrudates composed of ellagic acid /polymer (5/95% w/w) (plain lines), obtained in 0.1 N HCL with size 0 capsules containing 2 mg of EA.*

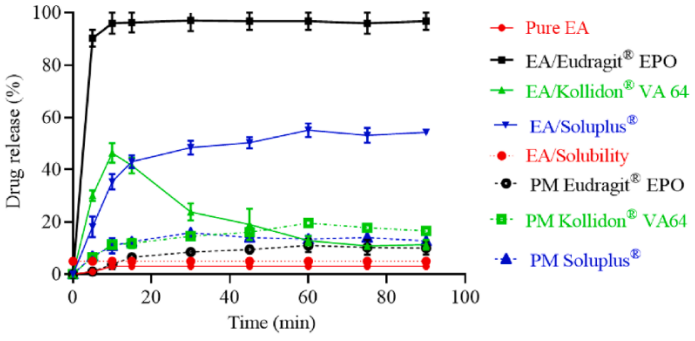

Fig. 8. *Effect of the increase of ellagic acid proportion in Eudragit® EPO on its dissolution profiles from extrudates with 5% w/w (black), 7.5% w/w (red), 10% w/w (blue) and 12% w/w (green) EA loading. These dissolution profiles were obtained in 0.1 N HCL with size 0 capsules containing 2 mg of ellagic acid. (For interpretation of the references to colour in this figure legend, the reader is referred to the web version of this article.)*

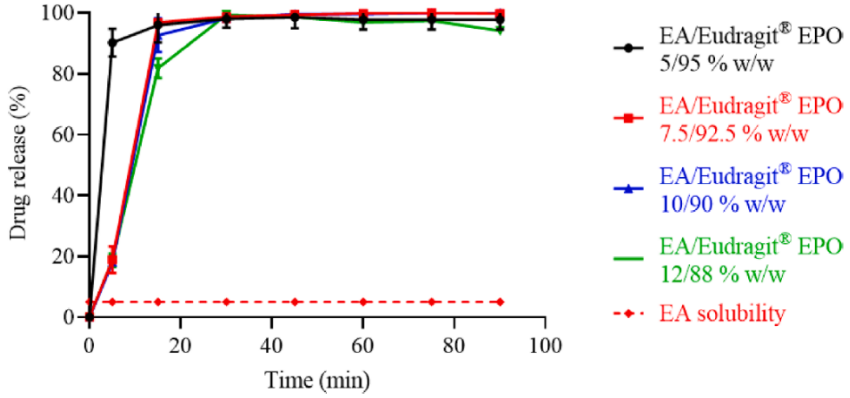

Fig. 9. *XRPD diffractograms of ellagic acid (black) and extrudates of ellagic acid / Eudragit® EPO 7.5/92.5% w/w (green), 10/90 % w/w (blue) and 12/ 88% w/w (red). (For interpretation of the references to colour in this figure legend, the reader is referred to the web version of this article.)*

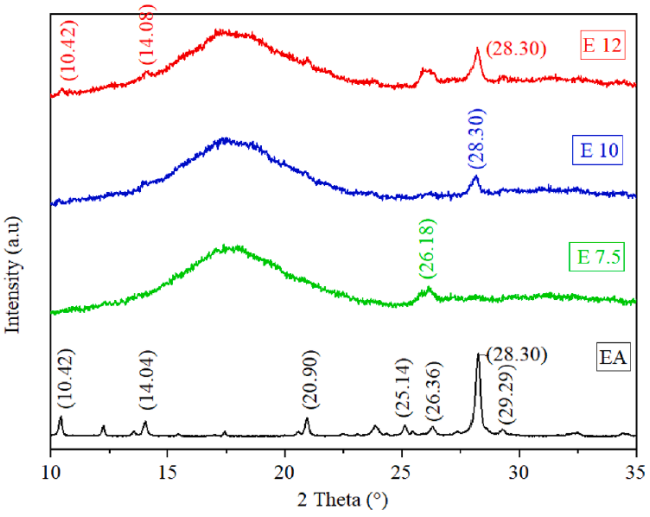

References

Alsulays, B.B., Park, J.B., Alshehri, S.M., Morott, J.T., Alshahrani, S.M., Tiwari, R.V., Alshetaili, A.S., Majumdar, S., Langley, N., Kolter, K., Gryczke, A., Repka, M.A., 2015. Influence of molecular weight of carriers and processing parameters on the extrudability, drug release, and stability of fenofibrate formulations processed by hot-melt extrusion. J. Drug Deliv. Sci. Technol. 29, 189–198. https://doi.org/ 10.1016/j.jddst.2015.07.011.

Anane-Adjei, A.B., Jacobs, E., Nash, S.C., Askin, S., Soundararajan, R., Kyobula, M., Booth, J., Campbell, A., 2022. Amorphous solid dispersions: Utilization and challenges in preclinical drug development within AstraZeneca. Int. J. Pharm. 614, 121387 https://doi.org/10.1016/j.ijpharm.2021.121387.

Anderson, B.D., 2018. Predicting Solubility / Miscibility in Amorphous Dispersions : It Is Time to Move Beyond Regular Solution Theories. J. Pharm. Sci. 107, 24–33. https:// doi.org/10.1016/j.xphs.2017.09.030.

Arulmozhi, V., Pandian, K., Mirunalini, S., 2013. Ellagic acid encapsulated chitosan nanoparticles for drug delivery system in human oral cancer cell line (KB). Colloids Surfaces B Biointerfaces 110, 313–320. https://doi.org/10.1016/j. colsurfb.2013.03.039.

Asati Amit, V., Salunkhe Kishor, S., Chavan Machindra, J., Chintamani Ravindra, B., Pratap, R.S.R., 2020. Solubility enhancement of BCS classified IV drug-apixaban by preparation and evaluation of mesoporous nanomatrix. Int. J. Res. Pharm. Sci. 11, 880–890. https://doi.org/10.26452/ijrps.v11i1.1910.

Avachat, A.M., Patel, V.G., 2015. Self nanoemulsifying drug delivery system of stabilized ellagic acid-phospholipid complex with improved dissolution and permeability. Saudi Pharm. J. 23, 276–289. https://doi.org/10.1016/j.jsps.2014.11.001.

Ayad, M.H., 2015. Rational formulation strategy from drug discovery profiling to human proof of concept Rational formulation strategy from drug discovery profiling to human proof of concept. Drug delivery 22 (6), 877–884. https://doi.org/10.3109/ 10717544.2014.898714.

Bala, I., Bhardwaj, V., Hariharan, S., Sitterberg, J., Bakowsky, U., Ravi Kumar, M.N.V., 2005. Design of biodegradable nanoparticles: A novel approach to encapsulating poorly soluble phytochemical ellagic acid. Nanotechnology 16, 2819–2822. https:// doi.org/10.1088/0957-4484/16/12/014.

Bala, I., Bhardwaj, V., Hariharan, S., Kumar, M.N.V.R., 2006. Analytical methods for assay of ellagic acid and its solubility studies. J. Pharm. Biomed. Anal. 40, 206–210. https://doi.org/10.1016/j.jpba.2005.07.006.

Dávalos, J.Z., Lima, C.F.R.A.C., Santos, L.M.N.B.F., Romero, V.L., Liebman, J.F., 2019. Thermochemical and structural studies of gallic and ellagic acids. J. Chem. Thermodyn. 129, 108–113. https://doi.org/10.1016/j.jct.2018.09.027.

Dell'Agli, M., Galli, G.V., Corbett, Y., Taramelli, D., Lucantoni, L., Habluetzel, A., Maschi, O., Caruso, D., Giavarini, F., Romeo, S., Bhattacharya, D., Bosisio, E., 2009. Antiplasmodial activity of Punica granatum L. fruit rind. J. Ethnopharmacol. 125, 279–285. https://doi.org/10.1016/j.jep.2009.06.025.

Djuris, J., Nikolakakis, I., Ibric, S., Djuric, Z., Kachrimanis, K., 2013. Preparation of carbamazepine-Soluplus® solid dispersions by hot-melt extrusion, and prediction of drug-polymer miscibility by thermodynamic model fitting. Eur. J. Pharm. Biopharm. https://doi.org/10.1016/j.ejpb.2012.12.018.

Emam, M.h.F., Taha, N.F., Emara, L.H., 2021. A novel combination of Soluplus® and Poloxamer for Meloxicam solid dispersions via hot melt extrusion for rapid onset of action—part 1: dissolution and stability studies. J. Appl. Pharm. Sci. 11, 141–150. https://doi.org/10.7324/JAPS.2021.110218.

Gallardo, D., Skalsky, B., Kleinebudde, P., 2008. Controlled release solid dosage forms using combinations of (meth)acrylate copolymers. Pharm. Dev. Technol. 13, 413–423. https://doi.org/10.1080/10837450802202098.

Ghosh, I., Vippagunta, R., Li, S., Vippagunta, S., 2012. Key considerations for optimization of formulation and melt-extrusion process parameters for developing thermosensitive compound. Pharm. Dev. Technol. 17, 502–510. https://doi.org/ 10.3109/10837450.2010.550624.

Göke, K., Lorenz, T., Repanas, A., Schneider, F., Steiner, D., Baumann, K., Bunjes, H., Dietzel, A., Finke, J.H., Glasmacher, B., Kwade, A., 2018. Novel strategies for the formulation and processing of poorly water-soluble drugs. Eur. J. Pharm. Biopharm. 126, 40–56. https://doi.org/10.1016/j.ejpb.2017.05.008.

Gottschalk, T., Özbay, C., Feuerbach, T., Thommes, M., 2022. Predicting Throughput and Melt Temperature in Pharmaceutical Hot Melt Extrusion. Pharmaceutics 14 (9), 1757.

Grignard, E., Taylor, R., McAllister, M., Box, K., Fotaki, N., 2017. Considerations for the development of in vitro dissolution tests to reduce or replace preclinical oral absorption studies. Eur. J. Pharm. Sci. 99, 193–201. https://doi.org/10.1016/j. ejps.2016.12.004.

Guan, J., Jin, L., Liu, Q., Xu, H., Wu, H., Zhang, X., Mao, S., 2019. Exploration of supersaturable lacidipine ternary amorphous solid dispersion for enhanced dissolution and in vivo absorption. Eur. J. Pharm. Sci. 139, 105043 https://doi.org/ 10.1016/j.ejps.2019.105043.

Guo, Z., Lu, M., Li, Y., Pang, H., Lin, L., Liu, X., Wu, C., 2014. The utilization of drug- polymer interactions for improving the chemical stability of hot-melt extruded solid dispersions. J. Pharm. Pharmacol. 66, 285–296. https://doi.org/10.1111/ jphp.12145.

Haser, A., Huang, S., Listro, T., White, D., Zhang, F., 2017a. An approach for chemical stability during melt extrusion of a drug substance with a high melting point. Int. J. Pharm. https://doi.org/10.1016/j.ijpharm.2017.03.070.

Haser, A., Huang, S., Listro, T., White, D., Zhang, F., 2017b. An approach for chemical stability during melt extrusion of a drug substance with a high melting point. Int. J. Pharm. 524, 55–64. https://doi.org/10.1016/j.ijpharm.2017.03.070.

Hou, Y., Shao, J., Fu, Q., Li, J., Sun, J., He, Z., 2017. Spray-dried nanocrystals for a highly hydrophobic drug: Increased drug loading, enhanced redispersity, and improved oral bioavailability. Int. J. Pharm. 516, 372–379. https://doi.org/10.1016/j. ijpharm.2016.11.043.

Huang, Y., Dai, W.-G., 2014. Fundamental aspects of solid dispersion technology for poorly soluble drugs. Acta Pharm. Sin. B 4, 18–25. https://doi.org/10.1016/j.apsb.2013.11.001.

Huang, D., Xie, Z., Rao, Q., Liamas, E., Pan, P., Guan, S., Zhang, Z.J., Lu, M., Li, Q., 2019. Hot melt extrusion of heat-sensitive and high melting point drug: Inhibit the recrystallization of the prepared amorphous drug during extrusion to improve the bioavailability. Int. J. Pharm. 565, 316–324. https://doi.org/10.1016/j. ijpharm.2019.04.064.

Hughey, J.R., Keen, J.M., Brough, C., Saeger, S., McGinity, J.W., 2011. Thermal processing of a poorly water-soluble drug substance exhibiting a high melting point: The utility of KinetiSol ® Dispersing. Int. J. Pharm. 419, 222–230. https://doi.org/ 10.1016/j.ijpharm.2011.08.007.

Hughey, J.R., Keen, J.M., Miller, D.A., Kolter, K., Langley, N., McGinity, J.W., 2013. The use of inorganic salts to improve the dissolution characteristics of tablets containing Soluplus®-based solid dispersions. Eur. J. Pharm. Sci. 48, 758–766. https://doi.org/ 10.1016/j.ejps.2013.01.004.

Hussein, M.Z., Al Ali, S.H., Zainal, Z., Hakim, M.N., 2011. Development of antiproliferative nanohybrid compound with controlled release property using ellagic acid as the active agent. Int. J. Nanomedicine 6, 1373–1383. https://doi.org/ 10.2147/ijn.s21567.

Iyer, R., Jovanovska, V.P., Berginc, K., Jaklič, M., Fabiani, F., Harlacher, C., Huzjak, T., Sanchez-Felix, M.V., 2021. Amorphous solid dispersions (ASDs): The influence of material properties, manufacturing processes and analytical technologies in drug product development. Pharmaceutics 13. https://doi.org/10.3390/ pharmaceutics13101682.

Jankovic, S., Tsakiridou, G., Ditzinger, F., Koehl, N.J., Price, D.J., Ilie, A.R., Kalantzi, L., Kimpe, K., Holm, R., Nair, A., Griffin, B., Saal, C., Kuentz, M., 2019. Application of the solubility parameter concept to assist with oral delivery of poorly water-soluble drugs – a PEARRL review. J. Pharm. Pharmacol. 71, 441–463. https://doi.org/ 10.1111/jphp.12948.

Janssens, S., Van den Mooter, G., 2009. Physical chemistry of solid dispersions. J. Pharm. Pharmacol. 61 (12), 1571–1586. https://doi.org/10.1211/jpp/61.12.0001.

Juppo, A.M., Boissier, C., Khoo, C., 2003. Evaluation of solid dispersion particles prepared with SEDS. Int. J. Pharm. 250, 385–401. https://doi.org/10.1016/S0378- 5173(02)00577-X.

Kanaujia, P., Poovizhi, P., Ng, W.K., Tan, R.B.H., 2015. Amorphous formulations for dissolution and bioavailability enhancement of poorly soluble APIs. Powder Technol. 285, 2–15. https://doi.org/10.1016/j.powtec.2015.05.012.

Kong, Y., Wang, W., Wang, C., Li, L., Peng, D., Tian, B., 2023. Supersaturation and phase behavior during dissolution of amorphous solid dispersions. Int. J. Pharm. 631, 122524 https://doi.org/10.1016/j.ijpharm.2022.122524.

LaFountaine, J.S., McGinity, J.W., Williams, R.O., 2016. Challenges and Strategies in Thermal Processing of Amorphous Solid Dispersions: A Review. AAPS PharmSciTech 17, 43–55. https://doi.org/10.1208/s12249-015-0393-y.

Li, B., Harich, K., Wegiel, L., Taylor, L.S., Edgar, K.J., 2013. Stability and solubility enhancement of ellagic acid in cellulose ester solid dispersions. Carbohydr. Polym. 92, 1443–1450. https://doi.org/10.1016/j.carbpol.2012.10.051.

Li, J., Lee, I.W., Shin, G.H., Chen, X., Park, H.J., 2015. Curcumin-Eudragit® e PO solid dispersion: A simple and potent method to solve the problems of curcumin. Eur. J. Pharm. Biopharm. 94, 322–332. https://doi.org/10.1016/j.ejpb.2015.06.002.

Li, J., Lee, I.W., Shin, G.H., Chen, X., Park, H.J., 2015. Curcumin-Eudragit® e PO solid dispersion: A simple and potent method to solve the problems of curcumin. Eur. J. Pharm. Biopharm. https://doi.org/10.1016/j.ejpb.2015.06.002.

Li, H., Zhang, M., Xiong, L., Feng, W., Williams, R.O., 2020. Bioavailability improvement of carbamazepine via oral administration of modified-release amorphous solid dispersions in rats. Pharmaceutics 12, 1–16. https://doi.org/10.3390/ pharmaceutics12111023.

Li, Y., Zhao, X., Zu, Y., Zhang, Y., Ge, Y., Zhong, C., Wu, W., 2015. Preparation and characterization of micronized ellagic acid using antisolvent precipitation for oral delivery. Int. J. Pharm. 486, 207–216. https://doi.org/10.1016/j. ijpharm.2015.03.071.

Li, Y., Zhang, Y., Dai, W., Zhang, Q., 2021. Enhanced oral absorption and anti- inflammatory activity of ellagic acid via a novel type of case in nanosheets constructed by simple coacervation. Int. J. Pharm. 594, 120131 https://doi.org/ 10.1016/j.ijpharm.2020.120131.

Liu, J., Cao, F., Zhang, C., Ping, Q., 2013. Use of polymer combinations in the preparation of solid dispersions of a thermally unstable drug by hot-melt extrusion. Acta Pharm. Sin. B 3, 263–272. https://doi.org/10.1016/j.apsb.2013.06.007.

Liu, X., Feng, X., Williams, R.O., Zhang, F., 2018. Characterization of amorphous solid dispersions. J. Pharm. Investig. 48, 19–41. https://doi.org/10.1007/s40005-017- 0361-5.

Liu, H., Wang, P., Zhang, X., Shen, F., Gogos, C.G., 2010. Effects of extrusion process parameters on the dissolution behavior of indomethacin in Eudragit® E PO solid dispersions. Int. J. Pharm. 383, 161–169. https://doi.org/10.1016/j. ijpharm.2009.09.003.

Luebbert, C., Huxoll, F., Sadowski, G., Van Den Mooter, G., Grohganz, H., 2017. Amorphous-amorphous phase separation in API/polymer formulations. Molecules 22, 1–17. https://doi.org/10.3390/molecules22020296.

Maniruzzaman, M., Boateng, J.S., Snowden, M.J., Douroumis, D., 2012. A Review of Hot- Melt Extrusion : Process Technology to Pharmaceutical Products. https://doi.org/ 10.5402/2012/436763.

Markopoulos, C., Andreas, C.J., Vertzoni, M., Dressman, J., Reppas, C., 2015. In-vitro simulation of luminal conditions for evaluation of performance of oral drug products: Choosing the appropriate test media. Eur. J. Pharm. Biopharm. 93, 173–182. https://doi.org/10.1016/j.ejpb.2015.03.009.

Matrose, N.A., Obikese, K., Belay, Z.A., Caleb, O.J., 2021. Jo ur na l P re of. Sci. Total Environ. 135907 https://doi.org/10.1016/j.jddst.2021.102559.

Mendonsa, N., Almutairy, B., Kallakunta, V.R., Sarabu, S., Thipsay, P., Bandari, S., Repka, M.A., 2020. Manufacturing strategies to develop amorphous solid dispersions: An overview. J. Drug Deliv. Sci. Technol. 55, 101459 https://doi.org/ 10.1016/j.jddst.2019.101459.

Meng, F., Dave, V., Chauhan, H., 2015a. Qualitative and quantitative methods to determine miscibility in amorphous drug-polymer systems. Eur. J. Pharm. Sci. 77, 106–111. https://doi.org/10.1016/j.ejps.2015.05.018.

Meng, F., Trivino, A., Prasad, D., Chauhan, H., 2015b. Investigation and correlation of drug polymer miscibility and molecular interactions by various approaches for the preparation of amorphous solid dispersions. Eur. J. Pharm. Sci. 71, 12–24. https:// doi.org/10.1016/j.ejps.2015.02.003.

Menjoge, A.R., Kulkarni, M.G., 2007. Mechanistic investigations of phase behavior in Eudragit®E blends. Int. J. Pharm. 343, 106–121. https://doi.org/10.1016/j. ijpharm.2007.05.033.

Moseson, D.E., Jordan, M.A., Shah, D.D., Corum, I.D., Alvarenga Jr, B.R., Taylor, L.S., 2020. Application and limitations of thermogravimetric analysis to delineate the hot melt extrusion chemical stability processing window. Int. J. Pharm. 590, 119916 https://doi.org/10.1016/j.ijpharm.2020.119916.

Nyamba, I., Lechanteur, A., Semdé, R., Evrard, B., 2021. Physical formulation approaches for improving aqueous solubility and bioavailability of ellagic acid: A review. Eur. J. Pharm. Biopharm. 159, 198–210. https://doi.org/10.1016/j. ejpb.2020.11.004.

Parikh, T., Gupta, S.S., Meena, A.K., Vitez, I., Mahajan, N., Serajuddin, A.T., 2015. Application of film-casting technique to investigate drug–polymer miscibility in solid dispersion and hot-melt extrudate. J. Pharm. Sci. 104 (7), 2142–2152. https://doi. org/10.1002/jps.24446.

Price, D.J., Nair, A., Kuentz, M., Dressman, J., Saal, C., 2019. Calculation of drug- polymer mixing enthalpy as a new screening method of precipitation inhibitors for supersaturating pharmaceutical formulations. Eur. J. Pharm. Sci. 132, 142–156. https://doi.org/10.1016/j.ejps.2019.03.006.

Psimadas, D., Georgoulias, P., Valotassiou, V., Loudos, G., 2012. Molecular Nanomedicine Towards Cancer. J. Pharm. Sci. 101, 2271–2280. https://doi.org/ 10.1002/jps.

Reitz, E., Vervaet, C., Neubert, R.H.H., Thommes, M., 2013. Solid crystal suspensions containing griseofulvin-Preparation and bioavailability testing. Eur. J. Pharm. Biopharm. 83, 193–202. https://doi.org/10.1016/j.ejpb.2012.09.012.

Repka, M.A., Battu, S.K., Upadhye, S.B., Thumma, S., Crowley, M.M., Zhang, F., Martin, C., McGinity, J.W., 2007. Pharmaceutical applications of hot-melt extrusion: Part II. Drug Dev. Ind. Pharm. 33, 1043–1057. https://doi.org/10.1080/ 03639040701525627.

Restrepo-Uribe, L., Ioannidis, N., del Pilar Noriega, M., 2019. Dissolution improvement of an active pharmaceutical ingredient in a polymer melt by hot melt extrusion. J. Polym. Eng. 39 (2), 186–196.

Rumondor, A.C.F., Ivanisevic, I., Bates, S., Alonzo, D.E., Taylor, L.S., 2009. Evaluation of drug-polymer miscibility in amorphous solid dispersion systems. Pharm. Res. 26, 2523–2534. https://doi.org/10.1007/s11095-009-9970-7.

Saboo, S., Moseson, D.E., Kestur, U.S., Taylor, L.S., 2020. Patterns of drug release as a function of drug loading from amorphous solid dispersions: A comparison of five different polymers. Eur. J. Pharm. Sci. 155, 105514 https://doi.org/10.1016/j. ejps.2020.105514.

Salmani, J.M.M., Lv, H., Asghar, S., Zhou, J., 2015. Amorphous solid dispersion with increased gastric solubility in tandem with oral disintegrating tablets: A successful approach to improve the bioavailability of atorvastatin. Pharm. Dev. Technol. 20, 465–472. https://doi.org/10.3109/10837450.2014.882938.

Sarode, A.L., Sandhu, H., Shah, N., Malick, W., Zia, H., 2013. Hot melt extrusion (HME) for amorphous solid dispersions: Predictive tools for processing and impact of drug- polymer interactions on supersaturation. Eur. J. Pharm. Sci. 48, 371–384. https:// doi.org/10.1016/j.ejps.2012.12.012.

Sarode, A.L., Obara, S., Tanno, F.K., Sandhu, H., Iyer, R., Shah, N., 2014. Stability assessment of hypromellose acetate succinate (HPMCAS) NF for application in hot melt extrusion (HME). Carbohydr. Polym. 101, 146–153. https://doi.org/10.1016/j.carbpol.2013.09.017.

Savic, I.M., Jocic, E., Nikolic, V.D., Popsavin, M.M., Srdjan, J., Savic-gajic, I.M., Savic, I. M., Jocic, E., Nikolic, V.D., Popsavin, M.M., 2019. The effect of complexation with cyclodextrins on the antioxidant and antimicrobial activity of ellagic acid. Pharm. Dev. Technol. 24, 410–418. https://doi.org/10.1080/10837450.2018.1502318.

Shadambikar, G., Kipping, T., Di-Gallo, N., Elia, A.G., Knüttel, A.N., Treffer, D., Repka, M.A., 2020. Vacuum compression molding as a screening tool to investigate carrier suitability for hot-melt extrusion formulations. Pharmaceutics 12, 1–17. https://doi.org/10.3390/pharmaceutics12111019.

Shah, S., Maddineni, S., Lu, J., Repka, M.A., 2013. Melt extrusion with poorly soluble drugs. Int. J. Pharm. 453, 233–252. https://doi.org/10.1016/j. ijpharm.2012.11.001.

Shamma, R.N., Basha, M., 2013. Soluplus®: A novel polymeric solubilizer for optimization of Carvedilol solid dispersions: Formulation design and effect of method of preparation. Powder Technol. 237, 406–414. https://doi.org/10.1016/j. powtec.2012.12.038.

Školáková, T., Souchová, L., Patera, J., Pultar, M., Školáková a, A., Zámostný, P., 2019. Prediction of drug-polymer interactions in binary mixtures using energy balance supported by inverse gas chromatography. Eur. J. Pharm. Sci. 130, 247–259. https:// doi.org/10.1016/j.ejps.2019.01.021.

Soh, P.N., Witkowski, B., Olagnier, D., Nicolau, M.L., Garcia-Alvarez, M.C., Berry, A., Benoit-Vical, F., 2009. In vitro and in vivo properties of ellagic acid in malaria treatment. Antimicrob. Agents Chemother. 53, 1100–1106. https://doi.org/ 10.1128/AAC.01175-08.

Spoerk, M., Koutsamanis, I., Kottlan, A., Makert, C., Piller, M., Rajkovaca, M., Paudel, A., Khinast, J., 2022. Continuous Processing of Micropellets via Hot-melt Extrusion. AAPS PharmSciTech 1–14. https://doi.org/10.1208/s12249-022-02405-7.

Tambosi, G., Coelho, P.F., Soares, L., Lenschow, I.C.S., Zétola, M., Stulzer, H.K., Pezzini, B.R., 2018. Challenges to improve the biopharmaceutical properties of poorly water-soluble drugs and the application of the solid dispersion technology. Rev. Mater. 23 https://doi.org/10.1590/s1517-707620180004.0558.

Thiry, J., Lebrun, P., Vinassa, C., Adam, M., Netchacovitch, L., Ziemons, E., Hubert, P., Krier, F., Evrard, B., 2016. Continuous production of itraconazole-based solid dispersions by hot melt extrusion:

Preformulation, optimization and design space determination. Int. J. Pharm. 515, 114–124. https://doi.org/10.1016/j. ijpharm.2016.10.003.

Thiry, J., Kok, M.G.M., Collard, L., Frère, A., Krier, F., Fillet, M., Evrard, B., 2017. Bioavailability enhancement of itraconazole-based solid dispersions produced by hot melt extrusion in the framework of the Three Rs rule. Eur. J. Pharm. Sci. 99, 1–8. https://doi.org/10.1016/j.ejps.2016.12.001.

Thommes, M., Ely, D.R., Carvajal, M.T., Pinal, R., 2011. Improvement of the dissolution rate of poorly soluble drugs by solid crystal suspensions. Mol. Pharm. 8, 727–735. https://doi.org/10.1021/mp1003493.

Tian, Y., Jacobs, E., Jones, D.S., McCoy, C.P., Wu, H., Andrews, G.P., 2020. The design and development of high drug loading amorphous solid dispersion for hot-melt extrusion platform. Int. J. Pharm. 586, 119545 https://doi.org/10.1016/j. ijpharm.2020.119545.

Tran, P.H.L., Lee, B.-J., Tran, T.T.D., 2021. Recent studies on the processes and formulation impacts in the development of solid dispersions by hot-melt extrusion. Eur. J. Pharm. Biopharm. 164, 13–19. https://doi.org/10.1016/j.ejpb.2021.04.009.

Tran, P., Park, J.S., 2021. Application of supercritical fluid technology for solid dispersion to enhance solubility and bioavailability of poorly water-soluble drugs. Int. J. Pharm. 610, 121247 https://doi.org/10.1016/j.ijpharm.2021.121247.

Tran, P., Pyo, Y.C., Kim, D.H., Lee, S.E., Kim, J.K., Park, J.S., 2019. Overview of the manufacturing methods of solid dispersion technology for improving the solubility and bioactivity in the hydroxyl radical oxidation system. Food Res. Int. 142, 110184 of poorly water-soluble drugs and application to anticancer drugs Pharmaceutics 11, https://doi.org/10.3390/pharmaceutics11030132.

Yuan, L., Mei, L., Guan, X., Hu, Y., 2021. Ellagic acid solid dispersion: Characterization. https://doi.org/10.1016/j.foodres.2021.110184.

Vo, C.L., Park, C., Lee, B., 2013. European Journal of Pharmaceutics and Biopharmaceutics Current trends and future perspectives of solid dispersions containing poorly water-soluble drugs. Eur. J. Pharm. Biopharm. 85, 799–813. https://doi.org/10.1016/j.ejpb.2013.09.007.

Wilson, M., Williams, M.A., Jones, D.S., Andrews, G.P., 2012. Hot-melt extrusion technology and pharmaceutical application. Ther. Deliv. 3, 787–797. https://doi. org/10.4155/tde.12.26.

Yuan, L., Mei, L., Guan, X., Hu, Y., 2021. Ellagic acid solid dispersion: Characterization and bioactivity in the hydroxyl radical oxidation system. Food Res. Int. 142, 110184 https://doi.org/10.1016/j.foodres.2021.110184.

Zazueta, C., 2015. Ellagic acid : Pharmacological activities and molecular mechanisms involved in liver protection 97, 84–103. https://doi.org/10.1016/j. phrs.2015.04.008.

Zhang, J., Yang, W., Vo, A.Q., Feng, X., Ye, X., Kim, D.W., Repka, M.A., 2017. Hydroxypropyl methylcellulose-based controlled release dosage by melt extrusion and 3D printing: Structure and drug release correlation. Carbohydr. Polym. 177, 49–57. https://doi.org/10.1016/j.carbpol.2017.08.058.

Zheng, Q., Zhang, Y., Montazerian, M., Gulbiten, O., Mauro, J.C., Zanotto, E.D., Yue, Y., 2019. Understanding Glass through Differential Scanning Calorimetry. Chem. Rev. 119, 7848–7939. https://doi.org/10.1021/acs.chemrev.8b00510.